Check for updates

Polyoxidovanadates $[Mo^{VI}V^V_9O_{28}]^{5-}$ and $[H_2Pt^{IV}V^V_9O_{28}]^{5-}$ interact with CHO cell plasma membrane lipids causing aggregation and activation of a G protein-coupled receptor

Kateryna Kostenkova[1†], Duaa Althumairy[2†], Ananthu Rajan[3], Ulrich Kortz[3], B. George Barisas[1,4], Deborah A. Roess[4,5]* and Debbie C. Crans[1,4]*

[1]Department of Chemistry, Colorado State University, Fort Collins, CO, United States, [2]Department of Biological Sciences, King Faisal University, Al-Ahsa, Saudi Arabia, [3]Department of Life Sciences and Chemistry, Jacobs University, Bremen, Germany, [4]Cell and Molecular Biology Program, Colorado State University, Fort Collins, CO, United States, [5]Department of Biomedical Sciences, Colorado State University Fort Collins, Fort Collins, CO, United States

Mono substituted heteropolyoxidovanadates, when compared to effects of a corresponding isopolyoxidovanadate (POV), were found to be more effective initiators of signal transduction by a G protein-coupled receptor (GPCR), specifically the luteinizing hormone receptor (LHR). Here we report that LHRs signal productively when CHO cells expressing the receptor are treated with two heteropolyoxidovanadates Pt^{IV} in monoplatino(IV)nonavanadate(V) ($[H_2Pt^{VI}V^V_9O_{28}]^{5-}$, V9Pt), and Mo^{IV} in monomolybdo(VI)nonavanadate(V) (Mo$[^{VI}V^V_9O_{28}]^{5-}$, V9Mo). Both substituted decavanadate derivatives were more effective than decavanadate which is more charged, has greater stability and forms the $[V_{10}O_{28}]^{6-}$ anion (V10) in cell culture medium at pH 7.4. For viable CHO cells expressing 10 k or 32 k LHR/cell and treated with 11 µM V9Pt and 13 µM V9Mo, mono substituted heteropolyoxidovanadates significantly decreased the packing of plasma membrane lipids for about 1 h. This brief change in membrane structure was accompanied by increased aggregation of LHR and cell signaling as indicated by increased intracellular levels of cAMP. More pronounced changes in lipid packing and LHR signaling were associated with short acting heteropolyoxidovanadates than with the more stable V10. When LHR was overexpressed, V9Pt and V9Mo had little or no effect on membrane lipid packing or receptor aggregation and the LHR was constitutively activated as indicated by elevated intracellular cAMP levels. Speciation of V9Pt and V9Mo in H_2O and cell medium was monitored using ^{51}V NMR spectroscopy and confirmed that V9Pt and V9Mo had greater effects on CHO cells despite decomposing more rapidly in the cell growth medium. Thus, under conditions that promote CHO cell growth, V9Pt and V9Mo, despite their smaller molecular charge and their reduced stability, favor LHR signaling over that induced by V10. Importantly, under the same experimental conditions, CHO cells treated with V9Pt and V9Mo do not exhibit as strong toxic effects observed for cells treated with the longer lived V10. In summary, unlike the longer lived V10 which is more growth inhibitory to cells, monosubstituted heteropolyoxidovanadates are more effective in transiently initiating signaling by a G protein-coupled receptor but, because of rapid hydrolysis, inhibit cell growth less.

1 Introduction

Polyoxidovanadates (POVs) are oxo-clusters containing octahedral vanadium metal ions vanadium oxo-cluster building blocks. These clusters are classified as homo- or heteropolyoxovanadates now also known as heteropolyoxidovanadates depending on whether their metal ion content is solely vanadium or vanadium with other metal ions. Isopolyoxidovanadates have specific nuclearities such as one, two, four, five, ten, 12 and 18 (Pope, 1983; Pope and Müller, 1991; Crans, 1994; Hill, 1998; Crans et al., 2004; Hayashi, 2011; Bijelic et al., 2019; Treviño and Diaz, 2020; Pessoa et al., 2021) and properties such as stability and redox potential that vary depending on their structures. Replacement of one of the metal ion with another metal provides a number of novel heteropolyoxidovanadates molecules with a wide range of properties. Recently studies of POVs (Mutlu et al., 2017; Samart et al., 2018; Sánchez-Lara et al., 2018; Treviño and Diaz, 2020; Treviño and González-Vergara, 2019; Aureliano et al., 2021; Aureliano et al., 2022) have shown that the anions were highly active and had biological properties that differed from the parent homopolyoxidometalate. Although some information is available on the interactions of isopolyoxidometalates with enzymes with distinct selectivity, there is little information comparing the biological effects of the POVs with heteropolyoxidovanadates and no consistent patterns identified for their effects (Crans, 1994). As examples, the isopolyoxidovanadates have more potent effects on glycerol-3-phosphate dehydrogenase and 6-phosphogluconate dehydrogenase activity (Crans, 1994), isopolyoxidomolybdates are more potent in their effects on glucose-6-phosphate dehydrogenase (Crans, 1993) and the heteropolyoxidovanadates are most potent in affecting recombinant and native reverse transcriptase activity (Yamamoto et al., 1992).

In this manuscript, we compare the effects of two monosubstituted isopolymetalates, two (POVs), monomolybdo(VI)nonavanadate(V) ([$^{VI}V^V_9O_{28}$]$^{5-}$, abbreviated V$_9$Mo) and monoplatino(IV)nonavanadate(V) ([$H_2Pt^{IV}V^V_9O_{28}$]$^{5-}$, abbreviated V$_9$Pt), with those of decavanadate ([$V_{10}O_{28}$]$^{6-}$, abbreviated V$_{10}$) on activation of luteinizing hormone receptors (LHR) expressed in Chinese hamster ovary (CHO) cells, a eukaryotic cell line. Comparing polyoxidometalates V$_9$Pt and V$_9$Mo effects on a eukaryotic cell membrane with V$_{10}$ is important because it begins to address structural features of these molecules necessary for their selective interaction with cell membranes is an isopolyoxidometalate that consists of ten octahedral vanadium (V) atoms, eight of which are bound to one terminal oxo ligand and five of those sharing oxygens in their octahedra (Figure 1) (Crans et al., 1994; Crans and Willsky, 1997; Aureliano and Crans, 2009). The last two vanadium atoms are internal and have six bridging oxygens in their octahedra. The V$_{10}$ structure is a compact ion and has the dimensions of 5.8 A˚ × 7.8 A˚ × 8.4 A˚ (Crans et al., 1994). Although the two POVs used in these studies are structurally similar to V$_{10}$, the replacement of one vanadium atom with either Pt^{IV} and Mo^{VI} results in a molecule with a different charge distribution and lower symmetry compared to the

all-V-containing V$_{10}$ (Figure 1). In the V$_9$Pt cluster, one of the two internal vanadium atoms is replaced by a platinum(IV) atom (Figure 1) and the charge on the V$_9$Pt ion is minus five due to the exchange of one central addenda site by a Pt^{IV} ion. The dimensions of V$_9$Pt (5.5 A˚ × 7.7 A˚ × 8.5 A˚) are similar to those of the V$_{10}$, calculated from XRD data (Crans et al., 1994; Uk Lee et al., 2008). The crystal structure shows the complex with a C$_{2v}$ point group symmetry, with two protons found on the polyanion located on oxygens bridging Pt and V (Uk Lee et al., 2008). These protons are key for the formation of a dimer, [$H_4(Pt^{IV}V_9O_{28})_2$]$^{10-}$, through four O-H···O hydrogen bonds. Although hydrogen bonds between two V$_9$Pt ions persist at ambient temperature after dissolving the polyanion salt in water, heating results in discrete V$_9$Pt ions (Uk Lee et al., 2008; Dugar et al., 2016). In the V$_9$Mo cluster, one of the surface vanadium atoms on the cluster is replaced by molybdenum (Sánchez-Lombardo et al., 2016). Single-crystal X-ray analysis of the polyoxidometalate [(CH$_3$)$_4$N]$_4$ [$H_2MoV_9O_{28}$] CI·6H$_2$O] has indicated that the molybdenum atom can occupy four different "capping" metal atom positions (Strukan et al., 1997). Although this structure is not deposited in the Cambridge Crystal Structure Database, we assume that the POM dimensions are very similar, because the Mo–O and V–O bond lengths are close in lenth. Despite the different molecular composition, the spectroscopic properties of V$_9$Pt, V$_9$Mo and V$_{10}$ vary as do their solubility and stability in the cell growth medium used in these studies.

Vanadium coordination complexes have been the focus of recent work in cell systems (Scalese et al., 2019; Treviño and Diaz, 2020; Pessoa et al., 2021; Loizou et al., 2021; He et al., 2020; Biswas et al., 2022; Ferretti and León, 2022; Ribeiro et al., 2022; Semiz, 2022; Althumairy et al., 2020a; Sahu et al., 2022). Our group has shown that bismaltolatodioxovanadium(IV) (BMOV) and polyoxidovanadates are able to initiate signaling by the luteinizing hormone receptor (LHR), a G-protein coupled receptor (GPCR) (Roess et al., 2008; Crans et al., 2011; Winter et al., 2012; Al-Quatati et al., 2013; Althumairy et al., 2020b; Althumairy et al., 2020c; Althumairy et al., 2020d; Samart et al., 2020). The hydrophobic coordination complexes appear to initiate LHR signaling through interactions of the coordination complex with the external surface of the cell membrane and potential penetration of the complex into the lipid bilayer (Althumairy

FIGURE 1
Polyhedral representations of [VO_4]$^{2-}$ (V$_1$) [$V_{10}O_{28}$]$^{6-}$ (V$_{10}$) [$H_2PtV_9O_{28}$]$^{5-}$ (V$_9$Pt) and [$Mo^{VI}V_9O_{28}$]$^{5-}$ (V$_9$Mo) showing molecular differences in these compounds at pH 7.4. The Pt is shown in maroon and the Mo is shown in green in the molecular structures.
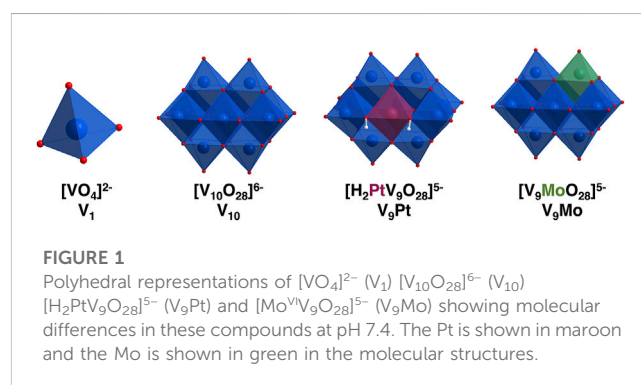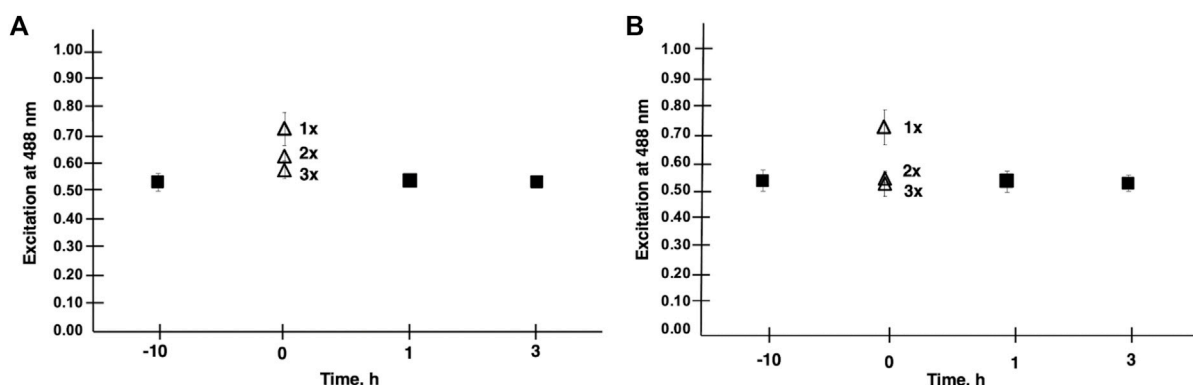
FIGURE 2
Membrane lipid order is shown in CHO cells treated with V_9Mo Panel **(A)** and V_9Pt Panel **(B)**. Results were obtained from the emission ratio of Di-4-ANEPPDHQ at 640/545 nm with excitation at 488 nm. A decrease in lipid order was indicated by increased emission at 640 nm relative to emission at 545 nm. The effects of washing cells with PBS a second (2 x) and third (3 x) time on lipid order was assessed at time 0 for both V_9Mo and V_9Pt. A second wash (2 x) increased lipid order and three washes (3 x) increased lipid order to values seen in untreated cells.

TABLE 1 Calculated values for the IC_{50} in Chinese Hamster Ovary (CHO) cells treated with V_9Pt and V_9Mo.

V-compound	IC_{50} per V-compound (μM)	IC_{50} per V-atom (μM)	Selected concentration for each V-compound (μM)
V_9Pt	12.9 ± 0.5	116 ± 5	10.0
V_9Mo	10.8 ± 0.6	97 ± 6	8.0

et al., 2020a; Samart et al., 2020, Winter et al., 2012; Crans et al., 2022). V_{10} is one of the POVs that has been found to be particularly potent in activation of LHR (Althumairy et al., 2020c) and the Type I Fc receptor (FcRI) (Al-Quatati et al., 2013). V_{10}, part of a class of polyoxometalates (polyoxidometalate) which are anionic metal-oxo clusters, has potential applications in the field of medicine (Pope and Müller, 1994; Rhule et al., 1998; Hasenknopf, 2005; Bijelic et al., 2018; Bijelic et al., 2019). Decametalates have anticancer and antidiabetic effects in eukaryotic cell lines and tissues and inhibit the growth of prokaryotic *Mycobacterium tuberculosis* mc2 6,230 (*M. tb*) and *Mycobacterium smegmatis* mc2 155 (*M. smeg* is now reclassified as a *Mycolicibacterium*) (Aureliano et al., 2021; Aureliano et al., 2022). Interestingly, in bacterial cell lines, inhibitory growth effects of V_{10} were greater than the effects of the known potent phosphatase inhibitor monovanadate (V_1) (Figure 1) (Samart et al., 2018; Kostenkova et al., 2021). The wide range of biological effects of decametalates in prokaryotic and eukaryotic cells motivates further work with these compounds given their potential pharmacologic value.

One mechanism of action used by several reported V-compounds is initiated through interactions of vanadium compounds with eukaryotic cell membranes either through intercalation or interactions at the membrane interface to alter the packing of plasma membrane lipids. Changes in lipid packing, in turn, drive the reorganization of the LHR in the membrane with receptors becoming concentrated in plasma membrane microdomains which function as signaling platforms for the receptor (Samart et al., 2018; Samart et al., 2020). Upon LHR aggregation, necessary for signal transduction by functional LHR, the receptor initiates intracellular

signaling, producing elevated intracellular levels of cAMP (Smith et al., 2006; Wolf-Ringwall et al., 2011). In the case of V_{10}, the mechanism of action is not likely to involve penetration or direct interaction of V_{10} at the membrane interface because the highly charged V_{10} polyanion remains outside the membrane. Of interest here are the biological effects of similar decametalates and, importantly, whether the lower charged V_9Mo and V_9Pt are capable of initiating albeit indirectly, LHR activation despite reduced stability compared to V_{10} in the eukaryotic cell medium.

2 Materials and methods

2.1 General materials

CHO-K1 cells were a kind gift from Dr. Takamitsu Kato at Colorado State University. Dulbecco's Modified Eagle medium (DMEM) with added geneticin was purchased from Corning Cellgro. Cell medium also contained penicillin/streptomycin and L-glutamine purchased from Gemini Bio-Products (West Sacramento, CA) and fetal bovine serum (FBS) purchased from Atlas Biologicals (Fort Collins, CO). The 100X MEM non-essential amino acid solution, sodium metavanadate ($NaVO_3$) and bovine albumin were from Sigma-Aldrich (St. Louis, MO). Trypsin-EDTA (0.25%) was supplied by Fisher Scientific Co. (Pittsburgh, PA), Optimal-MEM was obtained from Life Technologies (Carlsbad, CA). Glass-bottom cell culture dishes (CA35 mm diameter) used for optical measurements were obtained from *In Vitro* Scientific (Sunnyvale, CA).
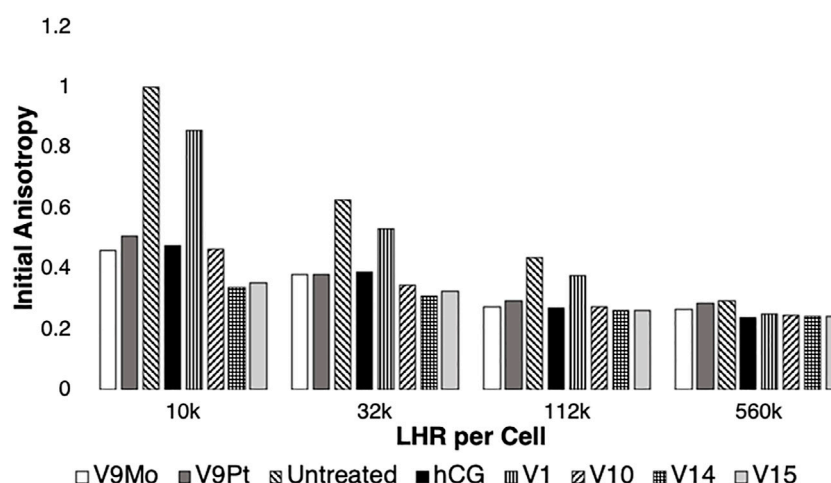
FIGURE 3
Data for treatment of the initial anisotropy measured for eYFP covalently linked to LHR using polarized homo-FRET methods was obtained by replotting data obtained in this work shown in Supplementary Figure S6 and combined with previous reported results (Althumairy et al., 2020c). The data is normalized relative to controls which were set to 1.0. Values for initial anisotropy less than 1.0 are indicative of LHR aggregation after treatment with V_9Pt and V_9Mo (this work) or with hCG, V_1, V_{10}, V_{14} or V_{15} as determined previously (Althumairy et al., 2020c). Pre-treatment of cells with hCG, V_1, V_9Pt, V_9Mo, V_{10}, V_{14} or V_{15} decreased values for initial anisotropy for LHR on cells expressing 10,000 or 32,000 LHR per cell plasma membranes. V_9Mo and V_9Pt had similar effect on LHR aggregation as did hCG and V_{10}. When cells expressed non-physiologically high numbers of LHR per cell (122,000 LHR/cell), receptors were already extensively aggregated. The conditions hCG, V_9Pt, V_9Mo, V_{10}, V_{14}, and V_{15} increased receptor aggregation while V_1 had no statistically significant effect on receptor clustering. There were no statistically significant effects of any treatment when CHO cells expressed 560,000 LHR per cell.

NaVO$_3$ and sodium molybdate (Na$_2$MoO$_4$) were purchased from Sigma Aldrich and used without purification. Monoplatinononavanadate ([H$_2$PtV$_9$O$_{28}$]$^{5-}$, abbreviated V$_9$Pt) the sodium salt was prepared as reported previously (Na$_5$ [H$_2$PtV$_9$O$_{28}$]· 21H$_2$O) (Uk Lee et al., 2008; Kostenkova et al., 2021). The peaks observed in ^{51}V NMR confirm the synthesis of the compound and are identical to those reported in the literature (Supplementary Figures S1-S2) (Uk Lee et al., 2008; Kostenkova et al., 2021). Monomolybdononavanadate ([MoV$_9$O$_{28}$]$^{5-}$) abbreviated V$_9$Mo) solution was freshly prepared following the reported procedure for the sodium salt (Na$_5$ [MoV$_9$O$_{28}$]·10H$_2$O) (Sánchez-Lombardo et al., 2016; Kostenkova et al., 2021). The peaks observed in ^{51}V NMR confirm the synthesis of the compound and were identical to those reported in the literature (Supplementary Figures S3-S4) (Sánchez-Lombardo et al., 2016; Kostenkova et al., 2021). The pH in NMR speciation experiments was adjusted by using either 0.1 M HCl or 0.1 M NaOH prepared in doubly deionized water (DDI) water.

2.2 Methods

2.2.1 NMR spectra
All NMR spectra were recorded using a Bruker NMR spectrometer at 105.2 MHz for ^{51}V, and a Varian NMR spectrometer at 131.5 MHz for ^{51}V at ambient temperature. Varian 500 MHz NMR spectrometer was manually calibrated by using a 5 mm broadband probe. The ^{51}V NMR spectra were recorded in DDI water (controls) and DMEM medium to determine speciation of V$_9$Mo and V$_9$Pt at several time-points

(0, 1, 5, 24, 30 and 48 h) during the experiment. The ^{51}V NMR spectra were recorded using the following parameters: 4,096 scans in the f1 domain, 0.01 s relaxation delay, O1p = –500 ppm, SW = 900 ppm, and a 16 μs pulse in a 45° pulse angle without lock and shimming turned on. The ^{51}V NMR spectra were reported relative to neat VOCl$_3$ at 0 ppm but experimentally referenced against an NaVO$_4$ solution at pH 12 (two signals one for V$_1$ at –535.7 ppm and the other for V$_2$ at –560.4 ppm) as an external reference) (Samart et al., 2018; Althumairy et al., 2020c). The MestreNova NMR processing software (version 14.0.1) was used for data processing.

2.2.2 Preparation of the stock solutions for speciation studies
The stock solution of V$_9$Pt (2.0 mM) was prepared by dissolving solid (0.0140 g, 0.0100 mmol) Na$_5$ [H$_2$PtV$_9$O$_{28}$]· 21H$_2$O in 5.00 ml DDI water. The stock solution of V$_9$Mo (2.0 mM) was prepared by using the desired volumes of DDI water and a 100 mM V$_9$Mo stock solution; the pH was adjusted to 5.0 by a dropwise addition of 0.1 M NaOH and 0.1 M HCl. The 1.0 mM control solutions of V$_9$Mo and V$_9$Pt were prepared by mixing 1,000 μL of the appropriate 2.0 mM stock solution with 1,000 μL of DDI H$_2$O. The 1.0 mM solutions of V$_9$Mo and V$_9$Pt in serum-free media prepared using the same method from 500 ml of DMEM, 5.0 ml of each penicillin/streptomycin, 100x non-essential amino acid solution, and L-glutamine solution. The pH of all solutions was measured at each indicated time-points (0, 1, 5, 24, 30 and 48 h) to determine possible changes in vanadium speciation during the 48h period of the experiment.
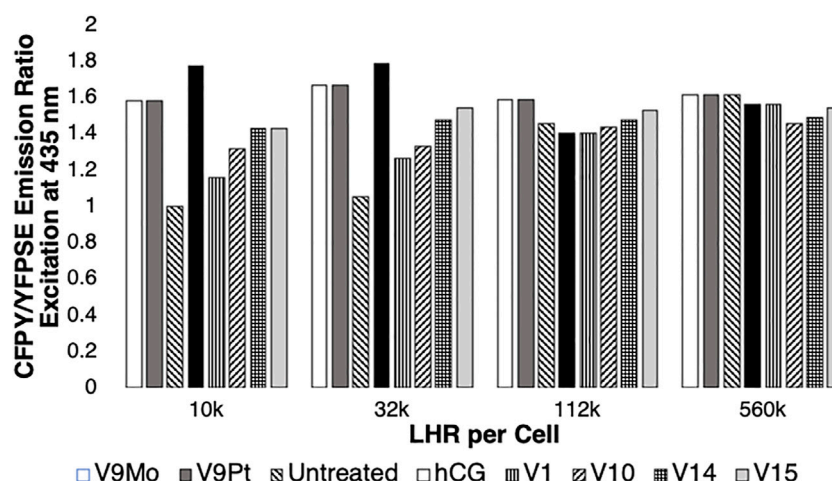
FIGURE 4
The effects of LHR numbers per cell on intracellular cAMP levels in the absence (untreated) or in the presence of cells treated with hCG, V_1, V_9Pt, V_9Mo, V_{10}, V_{10}, V_{14} or V_{15}. Data obtained in this work or reported previously (Althumairy et al., 2020c) is normalized with respect to the control value (1.0). An increase in intracellular cAMP is indicated by reduced energy transfer between CFP and YFP (YFPSE) upon exposure of ICUE3 to 435 nM light and an increase in the CFP/YFPSE ratio. Data shown from either this work or from a previous study (Althumairy et al., 2020c) are the mean of 25–43 individual measurements.

2.2.3 Preparation of the 1.0 mM V_9Pt solution with 0.11 M NaCl and 0.0054 M KCl for speciation studies

The 1.0 mM stock solution of V_9Pt with 0.11 M NaCl and 0.0054 M KCl was prepared by dissolving solid $Na_2[H_2PtV_9O_{28}]\cdot21H_2O$ (0.0070 g, 5.0 mmol), NaCl (0.032 g, 0.55 mmol) and KCl (0.0020 g, 0.027 mmol) in 90% H_2O/10% D_2O (4.5 ml DDI H_2O/0.5 ml D_2O). The pH of the solution was adjusted to 7 (pH = 7.4) with 0.05 M NaOH. The pH of the sample was measured at several time-points (0, 1, 5, 24, 30 and 48 h) to determine the changes in vanadium speciation over 48 h.

2.2.4 Effects of V_9Pt and V_9Mo on CHO cell viability

Cell growth was assessed using a resazurin-based fluorometric assay and serial diluted stock solutions of V_9Pt and V_9Mo into DMEM cell media as previously described (Althumairy et al., 2020c). Approximately 20,000 cells/well were seeded in 96-well plates in 100 µL free serum media. Cells were allowed to attach to plate surfaces for 3 h and then treated with solutions of 1.0, 5.0, 10, 50 or 100 µM of V_9Pt or V_9Mo together with 10% resazurin for 3 h to obtain a baseline value for cell viability (t = 0). A separate population of cells in 96 well plates were similarly treated for 12 h before the addition of 10% resazurin followed by an additional 3 h incubation (t = 15 h). Fluorescence measurements at t = 0 and t= 15 h were made using an excitation wavelength of 530 nm and measurement of fluorescence emission at 590 nm. The compound concentration where cell viability was 50% of the cell number at t = 0 was designated as the IC_{50} and was estimated by curve fitting to log values for both V_9Pt and V_9Mo (data not shown) to be 12.9 µM for V_9Pt and 10.8 µM for V_9Mo. The concentrations of V_9Pt and V_9Mo used in subsequent cell experiments, 10 µM and 8 µM, respectively, were less than the IC_{50} values for each compound

and were concentrations that were efficacious without causing high levels of cell death during the cell treatment.

2.2.5 V_9Pt and V_9Mo effects on CHO cell membrane lipid order

An environmentally sensitive styryl dye, di-4-ANEPPDHQ, was used to evaluate effects of V_9Pt and V_9Mo on membrane lipid order. This approach has been described in detail previously (Althumairy et al., 2020c). Briefly, CHO cells (0.5 ml) grown to at least 80% confluence in 50 ml cell culture flasks and treated with 1.0 ml trypsin-EDTA (0.25%) for 3 min were placed in a 35 mm glass-bottom Petri dish. After 12 h, cells were washed twice with phosphate-buffered saline (PBS) at pH 7.3 and then incubated in cell medium alone or in medium containing 10 µM V_9Pt or 8 µM V_9Mo. At time 0, a Petri dish containing CHO cells was labeled for 15 min with 200 µL of a stock solution containing 1.5 µM di-4-ANEPPDHQ before washing cells once, covering the cell layer with PBS and imaging cells (Althumairy et al., 2020b). Remaining Petri dishes were treated with 11 mM V_9Pt or 13 mM V_9Mo in media for 10 h, washed with PBS, covered in medium free serum and imaged at times 0, 1, and 3 h after labeling with di-4-ANEPPDHQ. The Zeiss Axiovert 200 M inverted microscope used for imaging was equipped with a 63 ×1.2 NA water objective and an Andor Du897 E EMCCD camera. Cell samples were illuminated using an arc lamp with a 480/30x or 495/20x excitation filter. Fluorescence emission was collected in channel one using a 535/40 nm filter and in channel two using a 620/40 nm filter and MetaFluor software. ImageJ software was used for background correction calculation of the fluorescence intensity ratio at 620nm/535 nm. Repeated cell washing was used in some experiments to evaluate the interactions of V_9Pt or V_9Mo with membrane lipids. As shown
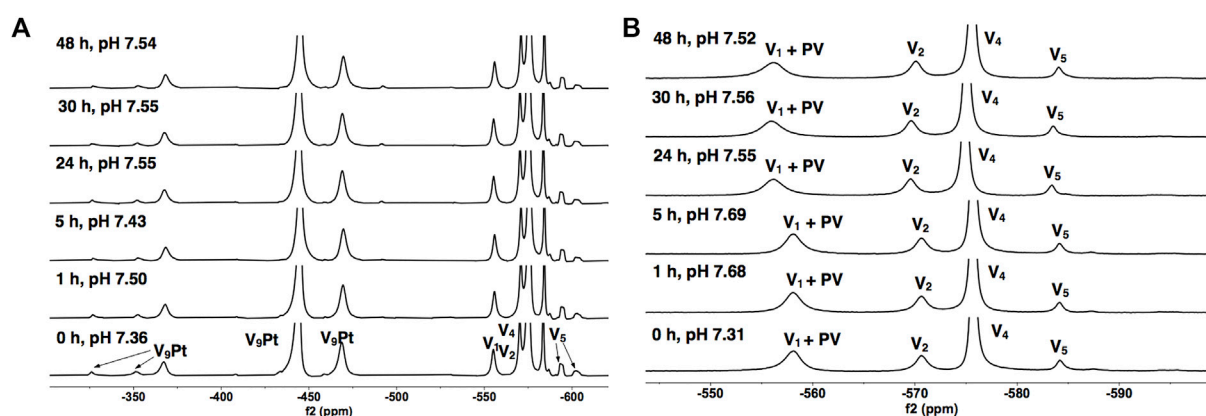
FIGURE 5
^{51}V NMR spectra of V$_9$Pt in **(A)** the 1.0 mM aqueous control solution and **(B)** the 1.0 mM solution in DMEM as a function of time. The signals (in ppm) are assigned to V$_9$Pt as follows: −379 (V$_D$), −445 (V$_{E/F}$) and −470 (V$_G$), a combined V$_1$ + PV signal (−573), V$_2$ (−571), V$_4$ (−575) and V$_5$ (-584 -592 and -602). The V$_9$Pt signals are identical to those reported in the literature (Kostenkova et al., 2021).

in Figure 2, cells at t=0 were washed two additional times designated 2x and 3x, prior to assessment of membrane lipid.

2.2.6 LHR aggregation determined by Polarized homo-fluorescence resonance energy transfer

The extent of LHR aggregation was determined using polarized homo-transfer fluorescence resonance energy transfer methods (referred to as homo-FRET) and performed as previously described (Althumairy et al., 2020c). Cells grown as described above were plated in 35 mm glass-bottom Petri dishes and allowed to attach to the glass surface for 12 h. Cells were then washed with PBS at pH 7.3 and treated for 10 h with solutions containing either 10 µ M V$_9$Pt or 8 µ M V$_9$Mo. After washing once to remove V$_9$Pt or V$_9$Mo, cells were covered with serum-free medium and imaged using homo-FRET protocols immediately at t = 0 or after further incubation for 1 h or 3 h, respectively (Althumairy et al., 2020c). At least five cells were examined from each Petri dish and a minimum of 30 cells were examined for each measured condition. Results are expressed as the mean ± SEM of individual measurements. Statistical evaluation of mean differences in untreated and treated groups were analyzed using a one-way ANOVA followed by the Tukey multiple comparison test and Student's t-test using R version 3.3.1. p values <0.05 were considered statistically significant.

2.2.7 Intracellular cAMP levels in V$_9$Pt- and V$_9$Mo-treated cells

Fluorescence assays of intracellular cyclic adenosine mono-phosphate (cAMP) were performed using a cAMP reporter ICUE3 expressed in CHO cells from an ICUE3 plasmid provided by Dr. Jin Zhang (DiPilato and Zhang, 2009) and methods in our laboratory that have been previously described in detail (Althumairy et al., 2020c). After transfection of CHO cells with the ICUE3 plasmid, images were acquired from cells in PBS to establish baseline levels of intracellular cAMP. The cell medium was then exchanged with solutions containing 10 µ M V$_9$Pt or 8 µ M V$_9$Mo. Cells were incubated for 15 min and reimaged. To

evaluate eYFP emission and eYFP sensitized emission (YFPSE) due to energy transfer from CFP, images were acquired used a 63 × 1.2 NA water objective in a Zeiss Axiovert 200 M inverted microscope with an Andor Du897 E EMCCD camera, arc lamp excitation with a 436DF20 excitation filter and two emission filters, 480DF40 for CFP and 535DF30. After background subtraction from the fluorescence images, data were analyzed using ImageJ software to calculate the emission intensity ratio of CFP/YFPSE. For each Petri dish, two to five cells were observed, and data were collected from a minimum of 15 cells for each treatment condition.

3 Results

3.1 Effects of V$_9$Mo and V$_9$Pt on lipid order in CHO cell plasma membranes

In initial experiments, we evaluated whether the water-soluble transition metal monosubstituted POVs, V$_9$Pt or V$_9$Mo, both less charged than V$_{10}$, had similar effects to those of V$_{10}$ on membrane lipid order. We have previously shown that V$_{10}$ decreases membrane lipid order in CHO cells for over 6 h (Althumairy et al., 2020c). Most previously investigated V-compounds are more hydrophobic coordination complexes and hence penetrate the membrane when exerting their function (Winter et al., 2012; Althumairy et al., 2020b), However, we found that in addiiton to V$_{10}$, V$_{14}$ ((K(NH$_4$)$_4$ [H$_6$V$_{14}$O$_{38}$(PO$_4$)]11H$_2$O)) and V$_{15}$ ([(CH$_3$)$_4$N]$_6$ [V$_{15}$O$_{36}$(Cl)]) had effects on membrane lipid order (Althumairy et al., 2020c). Initially we evaluated IC$_{50}$ values for V$_9$Pt or V$_9$Mo and, based on the IC$_{50}$, selected a lower concentration for each compound for use in subsequent experiments (Table 1). Lipid order in treated cells was decreased compared to untreated cells as indicated by an increase in the ratio of emission of di-4-ANEPPDHQ at 640/545 nm. After one washing of cells to remove excess V$_9$Pt or V$_9$Mo, lipid packing was evaluated at one or 3 h. At 1 h, lipid packing had returned to baseline values which

TABLE 2 Speciation data of the V_9Pt and V_9Mo clusters collected at t = 0, 24, and 48 h in 1.0 mM aqueous solutions (V_9Pt and V_9Mo), aqueous solution with added chloride anions and 1.0 mM solutions in DMEM media. No adjustments have been done to account for the polyoxidovanadates' hydrolysis.

Anions monitored	Signals observed by ^{51}V NMR spectroscopy								
Compound and time/ conditions	V_9Pt (%)	V_9Pt minor isomers (%)	V_9Mo (%)	V_{10} (%)	V_1 (%)	V_2 (%)	V_4 (%)	V_5 (%)	References
V_9Pt/0 h Aqueous Aq. With added Cl⁻Media	33.8% 7.9% 0%	1.1% 0.3% 0%	- - -	- - -	3.2% 7.5% V_1+PV 19.0%	5.4% 7.3% 10%	49.3% 68.0% 63.0%	7.0% 9.7% 7.0%	
V_9Pt/24 h Aqueous Aq. with added Cl⁻Media	33.0% 6.5% 0%	1.0% 0.3% 0%	- - -	- - -	3.1% 7.6% V_1+PV 20.0%	5.0% 8.5% 14.0%	51.2% 69.8% 63.0%	7.0% 8.2% 4.0%	
V_9Pt/48 h Aqueous Aq. with added Cl⁻Media	33.6% 6.1% 0%	0.3% 0.2% 0%	- - -	- - -	3.1% 7.5% V_1+PV 20.0%	5.4 6.7% 12.0	51.0% 70.4% 61.0%	5.1% 10.3% 5.0%	
V_9Mo/0 h Aqueous Media	- -	- -	17.5% 16.5%	9.5% 7.5%	74.0% V_1+PV 66.0%	4.0% 1.0%	0% 0%	0% 0%	
V_9Mo/24 h Aqueous Media	- -	- -	21.5% 0%	10.5% 0%	74.0% V_1+PV 94.0%	0% 4.0%	0% 3.0%	0% 0%	
V_9Mo/48 h Aqueous Media	- -	- -	18.0% 0%	6.0% 0%	77.0% V_1+PV 97.0%	0% 5.0%	0% 3.0%	0% 0%	
V_{10}/0 h Aqueous Media	- -	- -	- -	56.9 89.3	14.6 V_1+PV 7.54	10.7 2.11	17.6 1.05	0.21 -	Althumairy et al. (2020a)
V_{10}/24 h Aqueous Media	- -	- -	- -	47.3 5.00	13.7 V_1+PV 20.6	10.5 12.6	28.4 56.7	- 5.37	Althumairy et al. (2020b)

* PV = V(V) phosphate species.

** Considering the lack of stability of some polyoxidovanadates, the values given in Table 2 have been reported without adjusting for hydrolysis under assay conditions.

suggests that V_9Mo and V_9Pt effects on membrane lipid order were short lived. These results contrasted sharply with similar experiments with V_{10} where a single washing of V_{10} treated cells did not markedly affect membrane lipid order for at least 6 h (Althumairy et al., 2020c).

Because effects on membrane lipid order for V_9Pt and V_9Mo were short-lived, we evaluated the extent of V_9Pt and V_9Mo association with the membrane further by washing cells two additional times at time 0 as shown in Figure 2. Washing cells three times increased lipid packing to baseline values for both V_9Pt- and V_9Mo-treated cells indicating that these POVs exerted effects on membrane lipids while being only weakly associated with the cell membrane.

3.2 Aggregation of LHR

Effects of V_9Pt and V_9Mo treatment on LHR aggregation were examined using CHO cell lines stably expressing different levels of LHR receptors in the plasma membranes: 10,000 LHR, 32,000 LHR, 122,000 LHR or 560,0000 LHR, respectively (Figure 3 and Supplementary Figure S6). When cells expressed 10,000 or 32,000 LHR per cell, preincubation of cells with 10 µM V_9Pt or 8 µM V_9Mo produced significant aggregation of LHR and decreased lipid order in CHO cell membranes. As we have seen previously (Althumairy et al., 2020d), cells expressing higher, non-physiological numbers of LHR per cell have LHRs that are extensively aggregated. For cells with 122,000 LHR per cell, V_9Mo and V_9Pt caused modest but significant effects on receptor aggregation. For cells expressing 560,000 LHR per cell, there was no further aggregation of LHR when cells were treated with either V_9Pt

or V_9Mo suggesting that the constitutive LHR aggregation due to receptor overexpression on untreated cells was not affected by changes in lipid order as has been previously observed.

In Figure 3 the data from Supplementary Figure S6 on the effects of V_9Pt and V_9Mo treatment on LHR aggregation was replotted with previously reported data for cells expressing 10,000, 32,000, 122,000 or 560,000 LHR per cell and treated with V_1, V_{10}, V_{14} ($(K(NH_4)_4$ $[H_6V_{14}O_{38}(PO_4)]11H_2O)$) and V_{15} $(([(CH_3)_4N]_6$ $[V_{15}O_{36}(Cl)]))$ (Althumairy et al., 2020c). The control values (untreated cells) were very similar and Figure 7 shows that the initial anisotropies with V_9Pt or V_9Mo treatment were similar to those previously reported for V_{10}-treated cells. Interestingly, V_9Pt, V_9Mo and V_{10} are less effective when CHO cells express lower LHR receptor numbers per cell compared to the larger multivalent oxidometalates V_{14} and V_{15}. For CHO cells with higher LHR receptor numbers, the effects of these compounds are similar. This may be due simply to pre-existing and extensive clustering of LHR when receptor numbers are high; membrane aggregation as evaluated here or, for example, binding of human chorionic gonadotropin (hCG) to the receptor (Althumairy et al., 2020c) which has no notable effects on cells where receptors were already highly aggregated.

3.3 Effects of V_9Mo and V_9Pt on cAMP levels in CHO cells

A low intracellular level of cAMP is indicated by a low CFP/YFPSE emission ratio. As shown in Figure 4, when examining cells expressing 10,000 LHR per cell, the increase in intracellular cAMP was most apparent with V_9Mo or V_9Pt treatment. Untreated
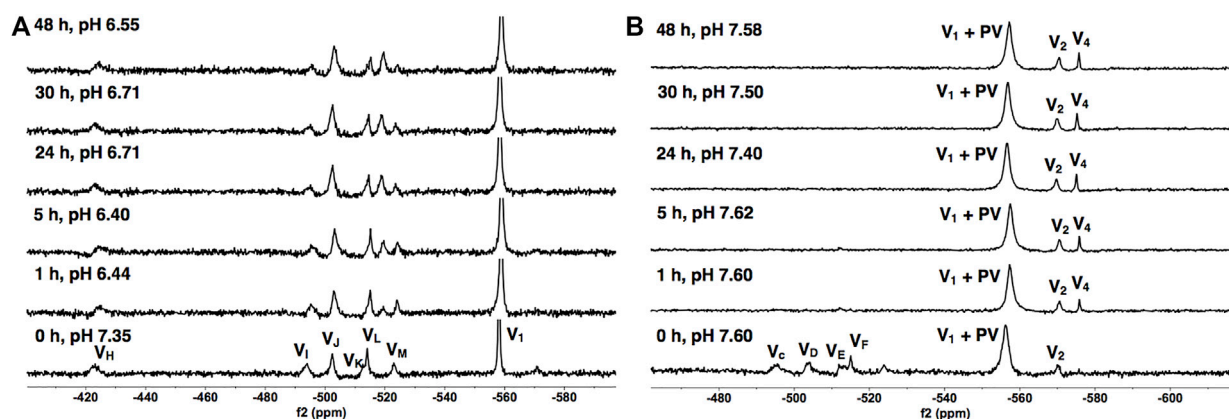
FIGURE 6
^{51}V NMR spectra of V_9Mo in **(A)** the 1.0 mM aqueous control solution and **(B)** the 1.0 mM solution in DMEM as a function of time. The signals (in ppm) are assigned (V_H, V_I, V_J, V_K, V_L and V_M = -423, -494, -503, -513, -515 and −523), the combined V1 + PV (−563) and V2 (−570). The V9Mo peaks are identical to those reported in the literature (Kostenkova et al., 2021).

receptors exhibit low basal levels of intracellular cAMP as indicated by the low ratio of CFP/YFPSE. However, as the number of LHR receptors increased the ratio of CFP/YFPSE increased showing that the levels of intracellular cAMP in untreated cells increases with increasing numbers of LHR per cell. Treating cells with either V_9Mo or V_9Pt significantly increased intracellular cAMP levels in CHO cells expressing 10,000 and 32,000 LHR expressed per cell. When cells overexpressed LHR, as shown in the experiments with either 122,000 or 560,000 LHR per cell, the addition of V_9Mo and V_9Pt had little or no effect on intracellular cAMP levels which were already high. These overexpressed receptors are pre-clustered, presumably due to high expression levels in the cell membrane, and, as a result, constitutively active as indicated by high levels of intracellular cAMP in untreated cells.

As shown in Figure 3, exposing CHO cells to either V_9Mo or V_9Pt caused anisotropy values to decrease, indicating LHR aggregation. There is a relationship between receptor clustering and intracellular levels of cAMP expressed by the CFP/YFPSE emission ratio shown in Figure 4. The increasing basal levels of intracellular cAMP in untreated cells with increasing numbers of LHR per cell were associated with decreasing initial anisotropies and plotted as 1.0. The data for V_9Mo or V_9Pt was plotted as the percentage of the control. Combining the data determined in this work and shown in Supplementary Figure S7 and plotted in Figure 4 with the data for hCG, V_1, V_{10}, V_{14} and V_{15}-treated CHO cells reported previously (Althumairy et al., 2020c) shows a similar pattern for hCG, V_1, V_9Pt and V_9Mo, V_{10}, V_{14} and V_{15}-treated cells expressing 10,000, 32, 000, 122,000, or 560,000 LHR per cell. In summary, receptors that were extensively clustered in response to the POVs described in this work or clustered as a result of LHR overexpression, were actively signaling as indicated by high cAMP levels. When considering cells expressing 10,000 LHR per cell, receptors needed to be activated by treatment of one of the V-anions. Figure 4 shows that V_9Pt and V_9Mo treatment produces a higher level of signaling than either hCG, a naturally occurring ligand for LHR, or any of the other V-containing compounds. Considering that V_9Pt and V_9Mo hydrolyze quickly,

this suggests that signaling happens very quickly after POVs are added to the assay solution. Moreover, the higher toxicity observed with V_{10} and higher multivalent POVs was not seen with V_9Pt and V_9Mo. In summary, V_9Pt and V_9Mo were both more effective in affecting membrane lipid organization and LHR-mediated cell signaling than the more stable, higher charged V_{10} and multivalent POV. These studies document that monosubstituted isopolymetalates are more efficacious as signaling agents while causing less toxicity than corresponding unsubstituted isopolymetalates.

3.4 Speciation and stability of V_9Pt and V_9Mo in H_2O and DMEM

Transition metal ion monosubstitution breaks the symmetry of V_{10}, resulting in different chemical shifts and relative signal intensities in ^{51}V NMR spectra, such as 2:4:4 in V_{10} to 1:6:2 in V_9Pt. Monosubstitution with Pt^{IV} in V_{10} results in four different types of vanadium atoms, for which two of the ^{51}V signals overlap, generating a total of three signals for the ^{51}V NMR spectrum of V_9Pt (V_D at -371.0, $V_{E/F}$ at -450.9, and V_G at -475.0 ppm) Figure 5. To assess V_9Pt speciation over the time course of cell studies, time-dependent ^{51}V NMR speciation studies of both V_9Pt and V_9Mo clusters were carried out in aqueous solutions and DMEM media at pH ≈ 7.4 over 48 h.

The ^{51}V NMR spectra in Figures 5A, B show that although the speciation of the V_9Pt in the aqueous solution with pH of 1.0 mM of V_9Pt maintained near pH 7.4 showed limited hydrolysis of PtV_9, the addition of PtV_9 to DMEM show extensive and immediate hydrolysis (Figure 5; Table 2). Overall, the ^{51}V NMR data indicates that the vanadate (V_1), forms rather quickly after dissolution of V_9Pt cluster in the media and that V_1 is the main component found in the media by the time sample is analyzed by ^{51}V NMR spectroscopy. The lack of stability in the DMEM media could be attributed to either higher pH (pH 7.4 rather than pH 6.6 in the Middelbrook 7H9 broth media used for cultivation of

TABLE 3 Calculated values for the IC_{50} in Chinese Hamster Ovary (CHO) cells treated with V_1, V_{10}, V_9Pt and V_9Mo.

V-compound	IC_{50} per V-compound (µM)	IC_{50} per V-atom (µM)	References
V_1 (Metallomics 2020)	56.7 ± 7.5	56.7 ± 7.5	Althumairy et al. (2020c)
V_{10} (Metallomics 2020)	3.2 ± 0.6	32 ± 6.0	Althumairy et al. (2020c)
V_9Pt	12.9 ± 0.5	129 ± 5	This work
V_9Mo	10.8 ± 0.6	108 ± 6	This work
V_{14}	6.1 ± 0.8	116 ± 5	Althumairy et al. (2020c)
V_{15}	8.2 ± 3.2	97 ± 6	Althumairy et al. (2020c)

mycobacteria), the higher concentrations of the chloride ions or other components in DMEM media. To determine whether the increased concentration of the chloride anions affects the stability of V_9Pt, we carried out a time-dependent ^{51}V NMR speciation experiment over 48 h with the added chloride anions (Supplementary Figure S5). The concentrations of the added NaCl and KCl are identical to those in the DMEM media (0.11 M and 0.0054 M, respectively) which are significantly higher than those in 7H9 media (0.015 M NaCl and 0.0045 mM KCl). The results shows that the speciation of the V_9Pt in the aqueous solution with the added chloride anion is indistinguishable from that observed to that in the aqueous control solution (Figures 5A and Supplementary Figure S5, Supplementary Tables S1 and Supplementary Figure S1), indicating that another component of the media causes immediate hydrolysis of V_9Pt. Overall, the ^{51}V NMR data indicates that the vanadate oligomers (V_1+PV, V_2, V_4, and V_5), rather than the V_9Pt cluster are the major species present in the DMEM media very quickly after dissolution of the V_9Pt.

To determine the speciation and stability of V_9Mo, we examined time-dependent ^{51}V NMR speciation over 48 h in H_2O and DMEM. The spectra of 1.0 mM of V_9Mo are shown in Figure 6. Transition metal ion monosubstitution breaks the symmetry in the V_{10}, resulting in different chemical shifts and relative intensities of the signals (2:4:4 in V_{10}, and 2:2:2:1:2:1 in V_9Mo). Monosubstitution with Mo^{VI} results in six different types of vanadium atoms with the following chemical shifts: V_H at -423 ppm, V_I at -494 ppm, V_J at -503 ppm, V_K at -513 ppm, V_L at -515 ppm, and V_M at –523 ppm. Additionally, V_H, V_I and V_J contain approximately 50% of V_9Mo and 50% V_{10} which was accounted for in all concentration calculations (Kostenkova et al., 2021).

The results of the spectroscopic studies of 1.0 mM V_9Mo aqueous control and 1.0 mM V_9Mo solution in DMEM at pH ≈ 7.4 are shown in Figures 6A, B, respectively. The ^{51}V NMR speciation data show that the V_9Mo cluster partially hydrolyzes in solution into the phosphovanadate (PV) derivative and vanadium oligomers (PV, V_1, V_2, V_4 and V_5) and small quantities of the V_9Mo isomer (-326 ppm and –352 ppm). The NMR data show that majority of the V_9Mo cluster hydrolyzes in the aqueous control solution at 0 h (17.5% of the sample), generating significant quantities of the phosphovanadate (PV) derivative and vanadate oligomers (74.0%). The amounts of both V_9Mo and V_1+PV remain unchanged during 48 h. Interestingly, a significant drop in the pH from 7.35 to 6.44 is observed after 1 h, yet it does not affect the stability of V_9Mo in an aqueous solution over time. The NMR

data in DMEM has shown that most of the V_9Mo cluster hydrolyzes immediately in the media with small quantities (0.165 mM) of V_9Mo present in solution at 0 h. V_9Mo completely hydrolyzes into PV complex and vanadate oligomers (V_1—70.0%, V_2—2.0%) within 1 h (Figure 6B; Table 2). Overall, the results indicate that PV and vanadate (V_1), rather than the V_9Mo cluster is the major components present in the media solution; what little V_9Mo remained in the media was quickly hydrolyzed.

In Table 2 we also list the speciation carried out and reported previously showing the stability of V_{10} both in aqueous solution and in media (Althumairy et al., 2020c). The V_{10} is initially present in both aqueous and media solution, and small amounts are present in aqueous solution and media even at 24 h. This is particularly relevant since some V_{10} is formed in the solution containing V_9Mo, affecting the observed effects by V_9Mo because a fraction of the active polyoxidovanadates is not V_9Mo. Indeed, V_{10} is known to exert many different activities including antidiabetic effects (Crans et al., 2019; Feng et al., 2022), mitochondrial function (Aureliano and Ohlin, 2014), having anticancer effects (Bijelic et al., 2018), showing activities against a range of bacteria include mycobacterial *tuberculosis* (Samart et al., 2018 (Aureliano et al., 2021; Aureliano et al., 2022) and other bacteria (Aureliano and Crans, 2009; Bijelic et al., 2018; Samart et al., 2018; Sánchez-Lara et al., 2018; Aureliano et al., 2021; Aureliano et al., 2022). In some studies, both V_1 and V_{10} have been investigated and V_{10} was found to be much more potent than V_1 (Samart et al., 2018). In this work, we explored the responses of a G coupled-protein receptor (GCPR), LHR, to two classes of water-soluble POMs structurally related to V_{10}, hence two monosubstituted decavanadates (V_9Pt and V_9Mo). All three POVs have similar core structures but distinct chemical properties due to transition-ion monosubstitution with either Pt^{IV} or Mo^{VI} which changes formal charges, hydrolytic and redox stability of the compact decametalate. In this work, We compared the all V-atom V_{10} to monosubstituted decavanadates with potential biological applications with respect to effects on growth inhibition and signaling by a G protein-coupled receptor (Aureliano and Crans, 2009; Althumairy et al., 2020a; Althumairy et al., 2020c; Aureliano et al., 2021). In Table 3 we summarize the observed growth effects of the V_9Pt and V_9Mo determined in this work and compare them to the effects reported previously on V_1 (vanadate monomer), V_{10} (pure decavanadate), and two multivalent POVs V_{14} $((K(NH_4)_4$ $[H_6V_{14}O_{38}(PO_4)]$ $11H_2O))$ and V_{15} $([(CH_3)_4N]_6$ $[V_{15}O_{36}(Cl)])$ (Althumairy et al., 2020c).
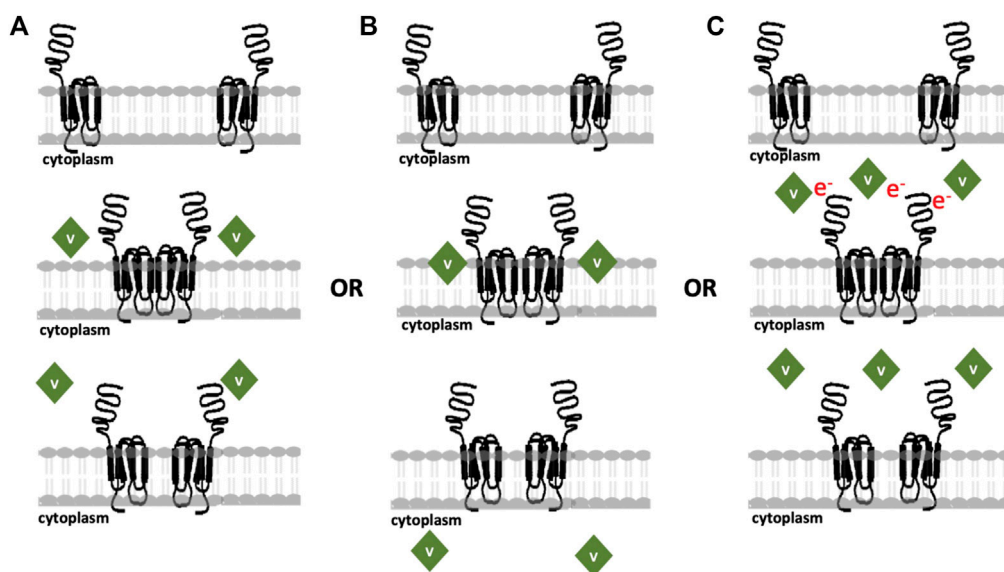
FIGURE 7
Updated proposed models for the modes of action of various vanadium compounds on cell membranes where cells express 10,000 LHR in plasma membrane per cell, at a comparatively low receptor density. **(A)** V-Compounds interact with CHO cell membranes and are not internalized; **(B)** V-compounds impact the lipid bilayer followed by POV hydrolysis and internalization of the resulting species; or **(C)** POVs exert the effects through an electron transfer process and no internalization is necessary for response. The image is adopted from (Althumairy et al., 2020c) with updates.

4 Discussion

To attribute the effects of the two POVs and compare their effects to those of V_{10} and V_1 and the two multivalent POVs, we examined the stability and speciation of V_9Pt and V_9Mo both in aqueous stock solution and DMEM media. We monitored the speciation using ^{51}V NMR spectroscopy and the species forming under the condition of the biological studies are summarized in Table 2. The replacement of one V-atoms in the V_{10} molecule cause a difference in overall charge from -6 for V_{10} to -5 for V_9Pt and V_9Mo whereas the structure of the decametalate remains very similar. Previous work has shown that V_9Pt is stable in the acidic bacterial media (Kostenkova et al., 2021) and that V_{10} partially hydrolyzes in DMEM over 10 h so we were surprised to see that V_9Pt hydrolyzed almost immediately in these studies. Similarly, the V_9Mo was found to hydrolyze within 1 h at the neutral pH values and medium used in this work which is faster than reported previously (Kostenkova et al., 2021). There are differences in the mediums use for bacterial 7H9 cells and eukaryotic CHO cells with higher Cl^- concentrations in 7H9 medium. To determine whether the reduced stability of V_9Pt in CHO cell growth medium could be attributed to Cl^- concentrations, we carried out time-dependent speciation experiments in an aqueous solution with added chloride anions (Supplementary Figure S5, Supplementary Table S1 and Supplementary Figure S1). The concentration of the added chloride salts produced a solution that was equivalent to that found in DMEM (0.0054 M KCl and 0.11 M NaCl). Since our results have shown that the stability and speciation of V_9Pt is identical in aqueous solutions with and without added chloride anions, we conclude that the lower stability of V_9Pt in this medium is caused by other factors which may include the various additives used

with mediums prepared for 7H9 and CHO cells as well as differences in the medium pH. For CHO cells studies, DMEM is supplemented with penicillin, streptomycin, L-glutamine, and protein-rich fetal bovine serum as well as geneticin to maintain stable expression of LHR in CHO cells. Any one of these additives or some combination of these additives may account for observed differences in V_9Pt stability when compared to studies of this molecule in bacterial cells. In addition, the possibility that any such species or a hydrolysis product of the V_9Pt or V_9Mo is an active species is very unlikely, since such species are not observed by ^{51}V NMR spectroscopy and therefore would be present at very low concentrations and hence very potent if such species was effective in initiating LHR signaling.

Some polyoxidometalates remain intact while others hydrolyze under the conditions of the biological studies, thus, carrying out speciation experiments under biological conditions is crucial to understanding their biological activities (Kiss et al., 2000; Bougie and Bisaillon, 2006; Postal et al., 2016; Levina et al., 2017; Levina and Lay, 2017; Nunes et al., 2021; Pessoa and Correia, 2021). Interestingly, growth inhibition of CHO cells by V_9Pt and V_9Mo is weaker than the growth inhibition observed for V_{10}-treated cells. A previous study of mixed valence POVs with LHR also investigated their stability and speciation at pH 7.4 using ^{51}V NMR and EPR spectroscopies. (Althumairy et al., 2020c). V_{15} is particularly interesting in that it contains 7 V (V) and 8 V (IV) and that part of its decomposition involves oxidation to the V_{15}—that is an all V (V) anion (Nunes et al., 2012; Postal et al., 2016). The results have therefore shown that V_{15} remains intact in DMEM at 0 and 24 h with the trace level of the reduced V (IV) species present until 24 h at ambient temperature EPR spectra (Althumairy et al., 2020c). V_{14}, in contrast, partially hydrolyzes starting at 0 h and is completely hydrolyzed at

24 h, as evidenced in the ambient temperature EPR spectra in DMEM (Althumairy et al., 2020c). The growth inhibition of V_9Pt and V_9Mo is also weaker than the growth inhibition observed for V_{14} and V_{15}. This is most readily understood if one considers that V_{10} and V_{15} are more stable than V_9Pt and V_9Mo. In the case of V_{14}, the situation is less obvious because this species easily decomposes. However, because both V_9Pt and V_9Mo are significantly more potent growth inhibitors than V_1, decomposition of these compounds to V_1 does not explain their observed effects on cell growth.

In this work, we investigated the effects on lipid order in CHO cells treated with V_9Mo and V_9Pt after repeated (three times) washings at t = 0. The lipid order was monitored measuring the emission at 640 nm relative to emission at 545 nm followed by excitation of the fluorophore with 488 nm light; decreased ratios is indicative of a decrease in lipid order. A decrease in the emission ratio after the first, the second (2 x) and the third (3 x) wash indicated increased lipid order compared to untreated cells (Figure 2). Because the extent of lipid packing returned to baseline values with repeated cell washing, it appears that these compounds have not penetrated the cells. Various experiments with either one cell wash or repeated cell washings were done previously for V_1, $VOSO_4$, BMOV and selected POVs-treated cells. With BMOV and $VOSO_4$ we showed that removing the V-compound with a single wash from cells with a low number of LHR per cell (10,000 LHR/cell) a greater increase in lipid packing was observed for the $VOSO_4$-treated cells compared to BMOV-treated cells (Althumairy et al., 2020a). After 24 h the lipid packing returned to levels near those of untreated cells suggesting that treatment with BMOV and $VOSO_4$ does not cause significant compound internalization.

Although studies using multiple cell washes have only recently been carried out, it is possible to compare the effects of single cell washes in cells treated with oxidovanadate and POVs with variable stabilities. V_1, V_{10} and V_{15} effects on lipid packing (Althumairy et al., 2020c) can be compared with those seen for V_9Mo-treated and V_9Pt-treated cells where cell treatment is followed by washing cells once. Under these conditions, V_1, V_{10} and V_{15} did not wash off cells as readily as did V_9Mo and V_9Pt which suggests that V_1, V_{10} and V_{15} are associated more closely with the membrane interface or, alternatively, that they are being at least partially internalized. Nonetheless, V_9Mo and V_9Pt can more effectively initiate LHR signaling; the observed increase in intracellular cAMP suggests that the signaling response must be very rapid despite hydrolyzing of V_9Mo and V_9Pt and that this rapid response is at least partially distinct from the more slowing developing effects on cell growth inhibition. It is likely that termination of LHR signaling in these experiments is due to the reestablishment of reduced membrane lipid packing, disaggregation of LHR and movement of LHR out of raft domains. Previous studies of LHR activated by the receptor ligand human chorionic gonadotropin (hCG), show that LHR become aggregated in membrane rafts and actively signal upon binding of hCG (Lei et al., 2007). Chemical disruption of the raft signaling platforms through cholesterol extraction from the plasma membrane is sufficient to eliminate signaling initiated by binding of hCG to LHR and LHR aggregation (Smith et al., 2006; Wolf-Ringwall et al., 2011). These studies led to the development of several mechanisms that are shown schematically in Figure 7 but do not rule out the possibility that vanadium compounds used in these experiments are interacting with the receptor.

Figure 7 shows various mechanisms previous proposed for the reported vanadium compounds interactions with cells that initiate signaling by LHR or other GCPRs. Because the POVs forms multiple species in media, it is likely that more than one type of interaction is taking place. Some species may interact with cells as shown in Figure 7A, while others use alternative mechanisms as summarized in Figure 7B or Figure 7C. For example, $VOSO_4$ and BMOV are likely to follow the mechanism illustrated in Figure 7B. However, washing experiments where one wash returns lipid organization to levels seen in untreated cells suggest that internalization is minimal (see (Althumairy et al., 2020a; Althumairy et al., 2020b), Figure 7A) demonstrates the interactions occurring for compounds like V_{14} and V_{15} and potentially V_9Mo and V_9Pt that interact with extracellular structures but due to their high hydrophilicity are unlikely to insert in lipid bilayers. Whether these compounds can perturb membrane structures or, as an example, alter LHR interactions with cholesterol (reviewed by (Sarkar and Chattopadhyay, 2020)), alter trafficking of this GPCR in the membrane as has been proposed for other Type A GPCRs (Weinberg and Puthenveedu, 2019) or indirectly increase homo-oligomerization of LHRs to activate signal transduction (Milligan et al., 2019) is not known. However, for hydrophilic compounds, interaction with the protein is likely to be responsible for some of the cellular changes in lipid packing that are observed.

Lipid bilayer interactions with lipophilic species and internalization of these V-compounds is an attractive alternative mechanism for lipophilic compounds that can penetrate the membrane. Many compounds and drugs must transit the plasma membrane, enter the cell cytoplasm before targeting intracellular structures (Chen et al., 2022). Transport of many compounds across a membrane depends on suitable membrane transporters that could facilitate the transport of specific compounds (Jafurulla et al., 2011). For example, the addition of DIDS stopped the internalization of V-compounds such as $VO(acac)_2$, BMOV and vanadate across erythrocyte membrane (Yang et al., 2003; Yang et al., 2004) but had no effect on transport of these same compounds in Caco-2 cells (Yang et al., 2004). These results demonstrate that a suitable transporter exists in erythrocytes but not in Caco-2 cells. Lipoidal diffusion is an alternative mechanism for drug movement across membrane barriers as described in detail in (Smith et al., 2014; McLauchlan et al., 2015). The mechanism shown in Figure 7C describe compounds that can weakly associate with the membrane-protein complex and initiate signaling though possible electron transfer. These compounds would be able to exert their mode of action without requiring internalization of the derivatives. Considering these mechanisms, it is important to determine the association of the compound with the membrane as well as whether internalization is taking place. V_1, V_{10}, V_{14} and V_{15}, as reported previously (Althumairy et al., 2020c), are associated with the cell membrane where they modulate membrane lipid packing and are not readily removed with 1 cell washing. This suggests some degree of internalization of these compounds at the membrane interface. In contrast, V_9Mo and V_9Pt are lost quickly from the cell membrane, a process that can be accelerated by washing cells repeatedly. These two compounds are examples of compounds that are not internalized and may act through mechanisms shown in Figures 7A, C.

5 Conclusion

These studies demonstrate that the interactions of two monosubstituted decavanadates, monoplatino(IV)nonavanadate(V) ($[H_2Pt^{VI}V^V_9O_{28}]^{5-}$, abbreviated V_9Pt, and monomolybdo(VI) nonavanadate(V) ($[Mo^{VI}V^V_9O_{28}]^{5-}$, abbreviated V_9Mo, with the eukaryotic cell plasma membrane directly decrease the packing of membrane lipids. The two monosubstituted decavanadates indirectly drive aggregation of LHR, a G protein-coupled receptor, in CHO cells when the receptor is not over-expressed in CHO cell membranes. These monosubstituted decavanadates are very effective in initiating LHR signaling, despite their hydrolytic instability and short life span under our assay conditions. This rapid signaling stands in contrast to the slower inhibitory effects on cell growth. The monosubstituted decavanadates therefore demonstrate selective signaling and lower toxicity manifested in terms of growth inhibition and since they hydrolyze fast and show less growth effects when compared to corresponding unsubstituted isopolyvanadates such as the decavanadate anion. In summary, $V_{10}O_{28}{}^{6-}$ is less efficient at initiating cell signaling while causing greater growth inhibition and hence cell toxicity. These studies have uncovered differences in cellular effects induced by decavanadate and monosubstituted derivatives V_9Pt and V_9Mo that may be of pharmacologic importance. Monosubstituted derivatives initiated a more rapid and greater signaling response that did V_{10}, possibly because of their structure and lower charge. Of benefit to cells, toxic effects of the monosubstituted derivatives are lessened because of their reduced stability compared to V_{10}.

Data availability statement

The original contributions presented in the study are included in the article/Supplementary Material, further inquiries can be directed to the corresponding authors.

Author contributions

Project conception DC and DR; Project management DR and DC; Experimental design DR, DA, DC, KK, and BB; Experiments DA, KK, and AR; Verification DR, DC, DA, KK, and UK; Manuscript preparation DR, DC, and KK; Editing DR, DC, KK, UK, BB, DA, and AR; Grant funding DC and DR. All authors helped edit and have approved the submitted manuscript.

Funding

Acknowledgments

Conflict of interest

The authors declare that the research was conducted in the absence of any commercial or financial relationships that could be construed as a potential conflict of interest.

Publisher's note

All claims expressed in this article are solely those of the authors and do not necessarily represent those of their affiliated organizations, or those of the publisher, the editors and the reviewers. Any product that may be evaluated in this article, or claim that may be made by its manufacturer, is not guaranteed or endorsed by the publisher.

Supplementary material

The Supplementary Material for this article can be found online at: https://www.frontiersin.org/articles/10.3389/fchbi.2023.1126975/full#supplementary-material

References

Al-Qatati, A., Fontes, F. L., Barisas, B. G., Zhang, D., Roess, D. A., and Crans, D. C. (2013). Raft localization of Type I Fcε receptor and degranulation of RBL-2H3 cells exposed to decavanadate, a structural model for V2O5. *Dalton Trans.* 42, 11912–11920. doi:10.1039/c3dt50398d

Althumairy, D., Murakami, H. A., Colclough, R., Barisas, B. G., Roess, D. A., and Crans, D. C. (2020a). *Vanadium catalysis*. London, United Kingdom: Publishers Royal Society of Chemistry. Chapter 21. Vanadium Compounds as Indirect Activators of a G Protein-coupled Receptor.

Althumairy, D., Murakami, H. A., Zhang, D., Barisas, B. G., Roess, D. A., and Crans, D. C. (2020b). Effects of vanadium(IV) compounds on plasma membrane lipids lead to G protein-coupled receptor signal transduction. *J. Inorg. Biochem.* 203, 110873. doi:10.1016/j.jinorgbio.2019.110873

Althumairy, D., Postal, K., Barisas, B. G., Nunes, G. G., Roess, D. A., and Crans, D. C. (2020c). Polyoxometalates function as indirect activators of a G protein-coupled receptor. *Metallomics* 12, 1044–1061. doi:10.1039/d0mt00044b

Althumairy, D., Roess, D. A., and Barisas, B. G. (2020d). Effects of luteinizing hormone receptor expression level on receptor aggregation and function. *Biophysical J.* 118, 95a. doi:10.1016/j.bpj.2019.11.680

Aureliano, M., and Ohlin, C. A. (2014). Decavanadate *in vitro* and *in vivo* effects: Facts and opinions. *J. Inorg. Biochem.* 137, 123–130. doi:10.1016/j.jinorgbio.2014.05.002

Aureliano, M., and Crans, D. C. (2009). Decavanadate (V10O286-) and oxovanadates: Oxometalates with many biological activities. *J. Inorg. Biochem.* 103, 536–546. doi:10.1016/j.jinorgbio.2008.11.010

Aureliano, M., Gumerova, N. I., Sciortino, G., Garribba, E., Mclauchlan, C. C., Rompel, A., et al. (2022). Polyoxidovanadates' interactions with proteins: An overview. *Coord. Chem. Rev.* 454, 214344. doi:10.1016/j.ccr.2021.214344

Aureliano, M., Gumerova, N. I., Sciortino, G., Garribba, E., Rompel, A., and Crans, D. C. (2021). Polyoxovanadates with emerging biomedical activities. *Coord. Chem. Rev.* 447, 214143. doi:10.1016/j.ccr.2021.214143

Bijelic, A., Aureliano, M., and Rompel, A. (2019). Polyoxometalates as potential next-generation metallodrugs in the combat against cancer. *Angew. Chem. Int. Ed.* 58, 2980–2999. doi:10.1002/anie.201803868

Bijelic, A., Aureliano, M., and Rompel, A. (2018). The antibacterial activity of polyoxometalates: Structures, antibiotic effects and future perspectives. *Chem. Commun.* 54, 1153–1169. doi:10.1039/c7cc07549a

Biswas, B. K., Biswas, N., Saha, S., Rahaman, A., Mandal, D. P., Bhattacharjee, S., et al. (2022). Interaction with bioligands and *in vitro* cytotoxicity of a new dinuclear dioxido vanadium(V) complex. *J. Inorg. Biochem.* 237, 111980. doi:10.1016/j.jinorgbio.2022.111980

Bougie, I., and Bisaillon, M. (2006). Inhibition of a metal-dependent viral RNA triphosphatase by decavanadate. *Biochem. J.* 398, 557–567. doi:10.1042/bj20060198

Crans, D. C., Smee, J. J., Gaidamauskas, E., and Yang, L. (2004). The chemistry and biochemistry of vanadium and the biological activities exerted by vanadium compounds. *Chem. Rev.* 104, 849–902. doi:10.1021/cr020607t

Crans, D. C., Brown, M., and Roess, D. A. (2022). Vanadium compounds promote biocatalysis in cells through actions on cell membranes. *Catal. Today* 388-389, 216–223. doi:10.1016/j.cattod.2020.07.027

Crans, D. C. (1994). Enzyme interactions with labile oxovanadates and other polyoxometalates. *Comments Inorg. Chem.* 16, 35–76. doi:10.1080/02603599408035851

Crans, D. C., Henry, L., Cardiff, G., and Posner, B. I. (2019). Developing vanadium as an antidiabetic or anticancer drug: A clinical and historical perspective. *Mater. Ions Life Sci.* 19. doi:10.1515/9783110527872-008

Crans, D. C. (1993). Interactions of oxovanadates and selected oxomolybdates with proteins. *Mol. Eng.* 3, 277–284. doi:10.1007/bf00999638

Crans, D. C., Mahroof-Tahir, M., Anderson, O. P., and Miller, M. M. (1994). X-Ray structure of (NH4)6(gly-gly)2V10O28.cntdot.4H2O: Model studies for polyoxometalate-protein interactions. *Inorg. Chem.* 33, 5586–5590. doi:10.1021/ic00102a036

Crans, D. C., Schoeberl, S., Gaidamauskas, E., Baruah, B., and Roess, D. A. (2011). Antidiabetic vanadium compound and membrane interfaces: Interface-facilitated metal complex hydrolysis. *J. Biol. Inorg. Chem. S.* 16, 961–972. doi:10.1007/s00775-011-0796-5

Crans, D. C., and Willsky, G. R. (1997). *Oxovanadate and oxomolybdate cluster interactions with enzymes and whole cells the Proceedings from the 25th Steenbock Symposium*. Madison, WI, United States: University of Wisconsin-Madison.

Dipilato, L. M., and Zhang, J. (2009). The role of membrane microdomains in shaping β2-adrenergic receptor-mediated cAMP dynamics. *Mol. Biosyst.* 5, 832–837. doi:10.1039/b823243a

Dugar, S., Izarova, N. V., Mal, S. S., Fu, R., Joo, H.-C., Lee, U., et al. (2016). Characterization of PtIV-containing polyoxometalates by high-resolution solid-state 195Pt and 51V NMR spectroscopy. *New J. Chem.* 40, 923–927. doi:10.1039/c5nj01242b

Favre, D., Harmon, J. F., Zhang, A., Miller, M. S., and Kaltashov, I. A. (2022). Decavanadate interactions with the elements of the SARS-CoV-2 spike protein highlight the potential role of electrostatics in disrupting the infectivity. *cycle, J. Inorg. Biochem.* 234, 111899. doi:10.1016/j.jinorgbio.2022.11189

Feng, B., Dong, Y., Shang, B., Zhang, B., Crans, D. C., and Yang, X. (2022). Convergent protein phosphatase inhibitor design for PTP1B and TCPTP: Exchangeable vanadium coordination complexes on graphene quantum dots. *Adv. Funct. Mater.* 32, 2108645. doi:10.1002/adfm.202108645

Ferretti, V. A., and León, I. E. (2022). An overview of vanadium and cell signaling in potential cancer treatments. *Inorganics* 10, 47. doi:10.3390/inorganics10040047

Hasenknopf, B. (2005). Polyoxometalates: Introduction to a class of inorganic compounds and their biomedical applications. *Front. Biosci.* 10, 275–287. doi:10.2741/1527

Hayashi, Y. (2011). Hetero and lacunary polyoxovanadate chemistry: Synthesis, reactivity and structural aspects. *Coord. Chem. Rev.* 255, 2270–2280. doi:10.1016/j.ccr.2011.02.013

He, Z., Han, S., Zhu, H., Hu, X., Li, X., Hou, C., et al. (2020). The protective effect of vanadium on cognitive impairment and the neuropathology of alzheimer's disease in APPSwe/PS1dE9 mice. *Front. Mol. Neurosci.* 13, 21. doi:10.3389/fnmol.2020.00021

Hill, C. L. (1998). Introduction: Polyoxometalates - multicomponent molecular vehicles to probe fundamental issues and practical problems. *Chem. Rev.* 98, 1–2. doi:10.1021/cr960395y

Jafurulla, M., Tiwari, S., and Chattopadhyay, A. (2011). Identification of cholesterol recognition amino acid consensus (CRAC) motif in G-protein coupled receptors. *Biochem. Biophysical Res. Commun.* 404, 569–573. doi:10.1016/j.bbrc.2010.12.031

Kiss, T., Kiss, E., Garribba, E., and Sakurai, H. (2000). Speciation of insulin-mimetic VO(IV)-containing drugs in blood serum. *J. Inorg. Biochem.* 80, 65–73. doi:10.1016/s0162-0134(00)00041-6

Kostenkova, K., Arhouma, Z., Postal, K., Rajan, A., Kortz, U., Nunes, G. G., et al. (2021). PtIV- or MoVI-substituted decavanadates inhibit the growth of Mycobacterium smegmatis. *J. Inorg. Biochem.* 217, 1–10. doi:10.1016/j.jinorgbio.2021.111356

Lee, U., Joo, H. C., Park, K.-M., Mal, S. S., Kortz, U., Keita, B., et al. (2008). Facile incorporation of platinum(IV) into polyoxometalate frameworks: Preparation of [H2PtIVV9O28]5 and characterization by 195Pt NMR spectroscopy. *Angew. Chem. Int. Ed.* 47, 793–796. doi:10.1002/anie.200703082

Lei, Y., Hagen, G. M., Smith, S. M., Liu, J., Barisas, G., and Roess, D. A. (2007). Constitutively-active human LH receptors are self-associated and located in rafts. *Mol. Cell. Endocrinol.* 260-262, 65–72. doi:10.1016/j.mce.2005.11.046

Levina, A., Crans, D. C., and Lay, P. A. (2017). Speciation of metal drugs, supplements and toxins in media and bodily fluids controls *in vitro* activities. *Coord. Chem. Rev.* 352, 473–498. doi:10.1016/j.ccr.2017.01.002

Levina, A., and Lay, P. A. (2017). Stabilities and biological activities of vanadium drugs: What is the nature of the active species? *Chem. Asian J.* 12, 1692–1699. doi:10.1002/asia.201700463

Loizou, M., Hadjiadamou, I., Drouza, C., Keramidas, A. D., Simos, Y. V., and Peschos, D. (2021). Vanadium(V) complexes with siderophore vitamin E-hydroxylamino-triazine ligands. *Inorganics* 9, 73. doi:10.3390/inorganics9100073

Mclauchlan, C. C., Peters, B. J., Willsky, G. R., and Crans, D. C. (2015). Vanadium-phosphatase complexes: Phosphatase inhibitors favor the trigonal bipyramidal transition state geometries. *Coord. Chem. Rev.* 301-302, 163–199. doi:10.1016/j.ccr.2014.12.012

Milligan, G., Ward, R. J., and Marsango, S. (2019). GPCR homo-oligomerization. *Curr. Opin. Cell. Biol.* 57, 40–47. doi:10.1016/j.ceb.2018.10.007

Mutlu, E., Cristy, T., Graves, S. W., Hooth, M. J., and Waidyanatha, S. (2017). Characterization of aqueous formulations of tetra- and pentavalent forms of vanadium in support of test article selection in toxicology studies. *Environ. Sci. Pollut. Res.* 24, 405–416. doi:10.1007/s11356-016-7803-x

Nunes, G. G., Bonatto, A. C., De Albuquerque, C. G., Barison, A., Ribeiro, R. R., Back, D. F., et al. (2012). Synthesis, characterization and chemoprotective activity of polyoxovanadates against DNA alkylation. *J. Inorg. Biochem.* 108, 36–46. doi:10.1016/j.jinorgbio.2011.11.019

Nunes, P., Correia, I., Cavaco, I., Marques, F., Pinheiro, T., Avecilla, F., et al. (2021). Therapeutic potential of vanadium complexes with 1,10-phenanthroline ligands, quo vadis? Fate of complexes in cell media and cancer cells. *J. Inorg. Biochem.* 217, 111350. doi:10.1016/j.jinorgbio.2020.111350

Chen, R.C., Kang, R., and Tang, D. (2022). The mechanism of HMGB1 secretion and release). *Exp. Mol. Sci.* 54, 91–102. doi:10.1038/s12276-022-00736-w

Pessoa, J. C., and Correia, I. (2021). Misinterpretations in evaluating interactions of vanadium complexes with proteins and other biological targets. *Inorganics* 9, 17. doi:10.3390/inorganics9020017

Pessoa, J. C., Santos, M. F. A., Correia, I., Sanna, D., Sciortino, G., and Garribba, E. (2021). Binding of vanadium ions and complexes to proteins and enzymes in aqueous solution. *Coord. Chem. Rev.* 449, 214192. doi:10.1016/j.ccr.2021.214192

Pope, M. T. (1983). *Heteropoly and isopoly oxometalates*. Berlin: Springer-Verlag.

Pope, M. T., and Müller, A. (1991). Polyoxometalate chemistry: An old field with new dimensions in several disciplines. *Angewandte Chemie Int. Ed. Engl.* 30, 34–48. doi:10.1002/anie.199100341

Pope, M. T., and Müller, A. (1994). *Polyoxometalates: From platonic solids to anti-retroviral activity*. Dordrecht: Springer.

Postal, K., Maluf, D. F., Valdameri, G., R¨Udiger, A. L., Hughes, D. L., De S´A, E. L., et al. (2016). Chemoprotective activity of mixed valence polyoxovanadates against diethylsulphate in *E. coli* cultures: Insights from solution speciation studies. *RSC Adv.* 6, 114955–114968. doi:10.1039/c6ra15826a

Rhule, J. T., Hill, C. L., Judd, D. A., and Schinazi, R. F. (1998). Polyoxometalates in medicine. *Chem. Rev.* 98, 327–358. doi:10.1021/cr960396q

Ribeiro, N., Bulut, I., Pósa, V., Sergi, B., Sciortino, G., Pessoa, J. C., et al. (2022). Solution chemical properties and anticancer potential of 8-hydroxyquinoline hydrazones and their oxidovanadium(IV) complexes. *J. Inorg. Biochem.* 235, 111932. doi:10.1016/j.jinorgbio.2022.111932

Roess, D. A., Smith, S. M. L., Winter, P., Zhou, J., Dou, P., Baruah, B., et al. (2008). Effects of vanadium-containing compounds on membrane lipids and on microdomains used in receptor-mediated signaling. *Chem. Biodiversity* 5 (8), 1558–1570. doi:10.1002/cbdv.200890144

Sahu, G., Patra, S. A., Mohanty, M., Lima, S., Pattanayak, P. D., Kaminsky, W., et al. (2022). Dithiocarbazate based oxidomethoxidovanadium(V) and mixed-ligand oxidovanadium(IV) complexes: Study of solution behavior, DNA binding, and anticancer activity. *J. Inorg. Biochem.* 223, 111844. doi:10.1016/j.jinorgbio.2022.111844

Samart, N., Althumairy, D., Zhang, D., Roess, D. A., and Crans, D. C. (2020). Initiation of a novel mode of membrane signaling: Vanadium facilitated signal transduction. *Coord. Chem. Rev.* 416, 213286. doi:10.1016/j.ccr.2020.213286

Samart, N., Arhouma, Z., Kumar, S., Murakami, H. A., Crick, D. C., and Crans, D. C. (2018). Decavanadate inhibits mycobacterial growth more potently than other oxovanadates. *Front. Chem.* 6, 519. doi:10.3389/fchem.2018.00519

Sánchez-Lara, E., Treviño, S., Sánchez-Gaytán, B. L., Sánchez-Mora, E., Eugenia Castro, M., Meléndez-Bustamante, F. J., et al. (2018). Decavanadate salts of cytosine and metformin: A combined experimental-theoretical study of potential metallodrugs against diabetes and cancer. *Front. Chem.* 6, 402. doi:10.3389/fchem.2018.00402

Sánchez-Lombardo, I., Baruah, B., Alvarez, S., Werst, K. R., Segaline, N. A., Levinger, N. E., et al. (2016). Size and shape trump charge in interactions of oxovanadates with self-assembled interfaces: Application of continuous shape measure analysis to the decavanadate anion. *New J. Chem.* 40, 962–975. doi:10.1039/c5nj01788b

Sarkar, P., and Chattopadhyay, A. (2020). Cholesterol interaction motifs in G protein-coupled receptors: Slippery hot spots? *Syst. Biol. Med.* 12 (4), e1481. doi:10.1002/wsbm.1481

Scalese, G., Machado, I., Correia, I., Pessoa, J. C., Bilbao, L., Pérez-Diaz, L., et al. (2019). Exploring oxidovanadium(iv) homoleptic complexes with 8-hydroxyquinoline derivatives as prospective antitrypanosomal agents. *New J. Chem.* 43, 17756–17773. doi:10.1039/c9nj02589h

Semiz, S. (2022). Vanadium as potential therapeutic agent for COVID-19: A focus on its antiviral, antiinflamatory, and antihyperglycemic effects. *J. Trace Elem. Med. Biol.* 69, 126887. doi:10.1016/j.jtemb.2021.126887

Smith, D., Artursson, P., Avdeef, A., Di, L., Ecker, G. F., Faller, B., et al. (2014). Passive lipoidal diffusion and carrier-mediated cell uptake are both important mechanisms of membrane permeation in drug disposition. *Mol. Pharm.* 11, 1727–1738. doi:10.1021/mp400713v

Smith, S. M. L., Lei, Y., Liu, J., Cahill, M. E., Hagen, G. M., Barisas, B. G., et al. (2006). Luteinizing hormone receptors translocate to plasma membrane microdomains after binding of human chorionic gonadotropin. *Endocrinology* 147, 1789–1795. doi:10.1210/en.2005-1046

Strukan, N., Cindric, M., and Kamenar, B. (1997). Synthesis and structure of [(CH3)4N]4[H2MoV9O28]Cl·6H2O. *Polyhedron* 16, 629–634. doi:10.1016/0277-5387(96)00316-6

Treviño, S., and Diaz, A. (2020). Vanadium and insulin: Partners in metabolic regulation. *J. Inorg. Biochem.* 208, 111094. doi:10.1016/j.jinorgbio.2020.111094

Weinberg, Z. Y., and Puthenveedu, M. A. (2019). Regulation of G protein-coupled receptor signaling by plasma membrane organization and endocytosis. *Traffic* 20, 121–129. doi:10.1111/tra.12628

Winter, P. W., Al-Qatati, A., Wolf-Ringwall, A. L., Schoeberl, S., Chatterjee, P. B., Barisas, B. G., et al. (2012). The anti-diabetic bis(maltolato)oxovanadium(iv) decreases lipid order while increasing insulin receptor localization in membrane microdomains. *Dalton Trans.* 41, 6419–6430. doi:10.1039/c2dt30521f

Wolf-Ringwall, A. L., Winter, P. W., Liu, J, Van Orden, A. K., Roess, D. A., and Barisas, B. G. (2011). Restricted lateral diffusion of luteinizing hormone receptors in membrane microdomains. *J. Biol. Chem.* 286, 29818–29827. doi:10.1074/jbc.m111.250969

Yamamoto, N., Schols, D., De Clercq, E., Debyser, Z., Pauwels, R., Balzarini, J., et al. (1992). Mechanism of anti-human immunodeficiency virus action of polyoxometalates, a class of broad-spectrum antiviral agents. *Mol. Pharmacol.* 42, 1109–1117.

Yang, X.-G., Wang, K., Lu, J., and Crans, D. C. (2003). Membrane transport of vanadium compounds and the interaction with the erythrocyte membrane. *Coord. Chem. Rev.* 237, 103–111. doi:10.1016/s0010-8545(02)00247-3

Yang, X.-G., Yang, X.-D., Yuan, L., Wang, K., and Crans, D. C. (2004). The permeability and cytotoxicity of insulin-mimetic vanadium compounds. *Pharm. Res.* 21, 1026–1033. doi:10.1023/b:pham.0000029293.89113.d5